

Review

# A Review on the Full Chain Application of 3D Printing Technology in Precision Medicine

Shenglin Wu <sup>1</sup>, Jinbin Zeng <sup>2</sup>, Haoxin Li <sup>2</sup>, Chongyang Han <sup>2</sup>, Weibin Wu <sup>2</sup>, Wenyi Zeng <sup>3</sup> and Luxin Tang <sup>4,\*</sup>

- <sup>1</sup> School of Intelligent Manufacturing and Electrical Engineering, Guangzhou Institute of Science and Technology, Guangzhou 510540, China; wushenglin@gzlg2.wecom.work
- <sup>2</sup> College of Engineering, South China Agricultural University, Guangzhou 510642, China; jinbinzeng@stu.scau.edu.cn (J.Z.); lihaoxin@stu.scau.edu.cn (H.L.); scauhancy@stu.scau.edu.cn (C.H.); wuweibin@scau.edu.cn (W.W.)
- <sup>3</sup> School of Innovation and Entrepreneurship, Guangdong AIB Polytechnic, Guangzhou 510507, China; wenyizeng@gdaib.edu.cn
- <sup>4</sup> Guangdong Industrial Robot Integration and Application Engineering Technology Research Center, Guangzhou Institute of Technology, Guangzhou 510540, China
- \* Correspondence: tangluxin@21cn.com

**Abstract:** Personalized precision medicine is a new direction for medical development, and advanced manufacturing technology can provide effective support for the development of personalized precision medicine. Based on the layered accumulation manufacturing principle, 3D printing technology has unique advantages in personalized rapid manufacturing, and can form complex geometric shape parts at low cost and high efficiency. This article introduces the application progress of 3D printing technology in medical models, surgical navigation templates, invisible aligners, and human implants, analyzes their advantages and limitations, and provides an outlook for the development trend of 3D printing technology in precision medicine.

**Keywords:** personalization; precision medicine; 3D printing technology; precision manufacturing; rapid manufacturing; full chain



**Citation:** Wu, S.; Zeng, J.; Li, H.; Han, C.; Wu, W.; Zeng, W.; Tang, L. A Review on the Full Chain Application of 3D Printing Technology in Precision Medicine. *Processes* **2023**, *11*, 1736. <https://doi.org/10.3390/pr11061736>

Academic Editors: Luis Puigjaner

Received: 12 April 2023

Revised: 18 May 2023

Accepted: 1 June 2023

Published: 6 June 2023



**Copyright:** © 2023 by the authors. Licensee MDPI, Basel, Switzerland. This article is an open access article distributed under the terms and conditions of the Creative Commons Attribution (CC BY) license (<https://creativecommons.org/licenses/by/4.0/>).

## 1. Introduction

Precision medicine is a new model that differs from traditional medicine, and it is a data-driven approach that considers various factors such as genetic differences, lifestyle, and environment of the population. It matches the molecular and pathological characteristics of the patient, providing personalized diagnosis and treatment strategies to achieve the ultimate goal of improving patient health [1]. The necessary condition for achieving precision medicine is the need for medical aids adapted to human physiological characteristics, whereas traditional medical devices cannot meet individualized needs and are expensive. Therefore, advanced manufacturing technologies are urgently needed in the future of personalized precision medicine to achieve cost reduction and efficiency improvement [2].

Three-dimensional printing technology, also known as additive manufacturing technology, is based on a digital 3D model. By slicing the digital model through software, the material is gradually stacked under computer control to obtain the part configuration [3]. Compared to traditional subtractive manufacturing processes (such as turning, milling, planing, grinding) and equal material manufacturing processes (such as forging, casting, welding), 3D printing technology can manufacture parts of any configuration at low cost and high efficiency. Three-dimensional printing technology itself has a digital gene and its entire process can be applied in precision medicine, including image acquisition, segmentation, modeling, printing, post-processing, and quality control, which can be referred to as full chain application. So, it has a wide range of market demand in the medical field, and its industrial scale continues to expand. According to the report of Acumen Research

and Consulting, the global market size of medical 3D printing applications was USD 2.8 billion in 2022. It is estimated that the market size will reach USD 11 billion by 2032, with a compound annual growth rate of 16.6% from 2023 to 2032. Currently, the sub-fields in which 3D printing technology is mainly applied in the medical field include medical devices, dentistry, human implants, drugs, and other derivative fields, and their application maturity is shown in Table 1. It can be seen that orthopedic implants, prostheses, and dental applications are the largest market application areas, and countries all over the world attach great importance to medical 3D printing technology and its applications. This article mainly focuses on the application research and analysis of medical models, surgical guides, invisible aligners, and human implants, and provides an outlook for the development trends.

**Table 1.** Three-dimensional printing technology in medical subdivision fields and development stages.

Stage	Medical Subdivision Fields
Relatively mature and commercialized development Clinical data accumulation research Laboratory research stage	Medical model, surgical guide plate, dental application High-performance orthopedic implants Functional tissue organ

## 2. Silicon Models

### 2.1. Three-Dimensional Printing Technology of Silicon

Silicone printing technology has been developed in response to the issue that traditional medical models made of single-material hard plastics lack the soft characteristics of human organs, which consist of 60–70% soft tissues. With the hardness of silicone as low as Shore 0A, its elasticity approximates that of soft tissues, allowing for better simulation of the structure of human organs. Three-dimensionally printed silicone models can be divided into indirect 3D printing and direct 3D printing. Indirect printing involves manufacturing molds using 3D printing technology, pouring liquid silicone into the molds, curing the silicone, and then removing the mold to complete the process. Simple geometric models can be produced using a single mold, while more complex models require multiple component molds [4–6]. Three-dimensional printing technologies that can be used for mold-making include stereolithography (SLA) [7], selective laser sintering (SLS) [8], material jetting (MJ) [9,10], and fused deposition modeling (FDM) [11]. Regarding the characteristics of the indirect printing process, it is suitable for the mass production of high-resolution models. However, personalized manufacturing is required for medical models that simulate human organs due to the unique physiological features of each patient, which is not suitable for mass production. As silicone casting of medical models requires different molds for different patients, this approach extends production time and reduces efficiency.

Compared with indirect printing, direct 3D printing of silicone technology provides the possibility of the personalized printing of silicone medical models. However, the low viscosity, long curing time, and low elastic modulus characteristics of silicone materials present significant challenges for the 3D printing of silicone. Currently, 3D printing technologies that can be directly used to manufacture silicone models include material jetting [12–14], binder jetting [15], hybrid methods [16,17], vat polymerization [18,19], and material extrusion [20], among others. Their main technical characteristics are shown in Table 2, and this article introduces several commonly used 3D printing technologies.

**Table 2.** The characteristics of direct 3D printing of silicone technology.

3D Printing Method	Curing System	Advantages	Shortcomings
Vat Photopolymerization	UV	High resolution	Limit to the low-viscosity silicon
Material Jetting	UV or HTV	High speed Multi-color printing	Complex device structure

Table 2. Cont.

3D Printing Method	Curing System	Advantages	Shortcomings
Direct Ink Writing	UV or HTV	Simple structure	Poor equality and difficult to control
Removable Embedded 3D printing	UV or HTV	Low-viscosity ultra-soft materials printing	High interfacial tension
Complete Matrix-Cure Embedded 3D Printing	UV or HTV	Complex structure printing	Tedious steps

### 2.1.1. Vat Photopolymerization

Photopolymerization utilizes ultraviolet light or a laser as the light source, which is focused into a beam. With the help of a reflective galvanometer, the beam scans in the XY plane to guide the liquid material to rapidly undergo a photopolymerization reaction and transform from a liquid to a solid under light exposure. Photopolymerization 3D printing technologies include stereolithography (SLA) and continuous liquid interface production (CLIP), which have the advantages of high resolution. However, when using this process to print silicone products, it is important to ensure appropriate material viscosity to guarantee the removal of uncured liquid material from the model after printing. Additionally, suitable material viscosity helps to form a layer with a uniformly structured surface, enabling the next layer to be smoothly and efficiently cured on top of the previous layer. Nevertheless, the technology for high-viscosity silicone photopolymerization is still in its early stages. Kim et al. [21] presented a modified stereolithography (SLA) technique for producing silicone components from precursors that exhibit high viscosity. In this study, the 3D structure is fabricated via laser curing of the photopolymer within the vat, rather than on its surface. The proposed approach eliminates movement within the resin vat, leading to a hydrostatic environment that functions as a support structure. This fabrication technique, which does not rely on support structures, requires a highly advanced optics system and a low-power UV curing mechanism referred to as low one-photon polymerization (LOPP), which enables precise control over light intensity. Despite its current developmental stage, this approach has the potential to significantly enhance the three-dimensional (3D) printing of soft materials with future refinements.

In order to improve the feasibility of silicone materials produced using photopolymerization, Bhattacharjee et al. [22] developed a photosensitive polydimethylsiloxane (PDMS) material with mechanical properties comparable to commercially available Sylgard 184 (Dow Corning) for microfluidic applications. The team utilized a desktop digital light processing (DLP) printer featuring exceptional vertical and lateral resolution of 50  $\mu\text{m}$ , demonstrating its efficacy in the production of microfluidic devices. In another study, Wallin et al. [23] successfully prepared a silicone double network (SiLDN) by mixing photoresponsive thiolene with conventional RTV silicone, which is compatible with stereolithography (SLA) 3D printing. This material exhibited a low elastic modulus ( $E_{100\%} < 700 \text{ kPa}$ ), high ultimate strain ( $dL/L_0 < 400\%$ ), high toughness ( $U \sim 1.4 \text{ MJ}\cdot\text{m}^{-3}$ ), and high strength ( $\sigma \sim 1 \text{ MPa}$ ). This technique was applied to surgical training and biomedical engineering, where a heart model similar in proportion to a baby's heart was printed to simulate complex surgical conditions, as shown in Figure 1. Recently, fabricating silicone structure using vat photopolymerization has been commercially applied. Spectroplast (2022) has developed a silicone 3D printer known as SAM (Silicone Additive Manufacturing), which is based on photopolymerization technology and employs a range of photosensitive organosilicon materials possessing Shore hardness values ranging from 0A to A80. This technology substantially elevates design versatility for silicone models and enables the printing of heart valve models.

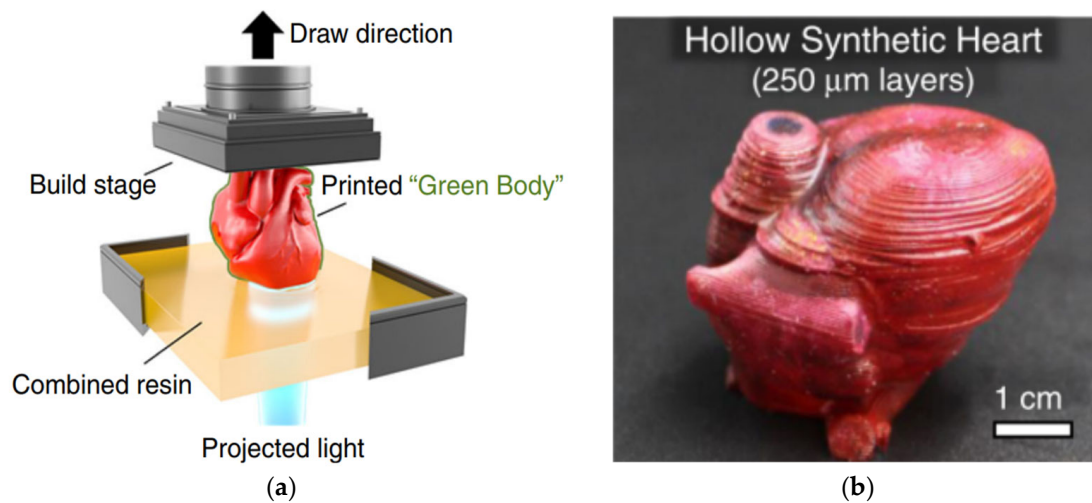


**Figure 1.** This picture is cited from “3D Printable Tough Silicone Double Networks” [23]. This picture shows that silicon heart models can be made via SLA. (a) The process of SLA; (b) the hollow synthetic heart.

### 2.1.2. Material Jetting

Material jetting is a 3D printing technology in which material is ejected from a small diameter nozzle in droplet form, layer by layer, to build up parts on a printing platform. The material is then cured using ultraviolet (UV) light, as shown in Figure 2. This technology can be combined with multi-color printing to produce stable multi-colored medical models. Additionally, a multi-nozzle structure can be designed [24]. The printing nozzle can be modified based on the rheological properties of the viscoelastic materials, and the characteristics of the raw materials used in the equipment can also be adjusted.

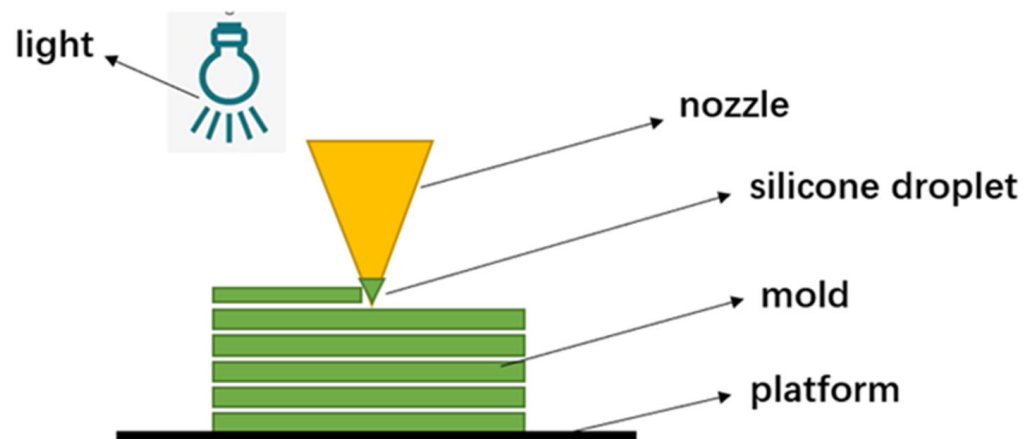


**Figure 2.** Material jetting.

Drop-on-demand technology is one type of material jetting using an inkjet head to deposit droplets of silicone onto a work platform, which then fuse together to form a homogeneous organic silicone layer. After each layer of organic silicone is printed, the system immediately uses ultraviolet light to cure the entire organic silicone layer. By using supporting materials to create complex structures such as holes, three-dimensional objects can be printed layer by layer. Once the printing is completed, the object is removed from the work platform and the supporting material is washed away with water. Subsequently, the object is subjected to a secondary vulcanization process to remove volatiles and achieve final mechanical properties.

The most prevalent types of actuation for drop-on-demand (DOD) printing heads are thermal and piezoelectric. In the case of thermal print heads, a resistor generates heat that rapidly produces a vapor bubble within the material reservoir, expelling a small volume of material from the nozzle as a droplet. While this process has the potential to elevate the local temperature of the material reservoir adjacent to the resistor over a brief timeframe and across a limited contact area, it may lead to degradation in thermo-labile active compounds. As such, thermal print heads are typically only suitable for high vapor pressures or volatile solvents. Alternatively, piezoelectric print heads incorporate piezoelectric components that produce mechanical motion in response to an electrical current. This process of deformation generates sufficient pressure to expel the liquid as droplets through the nozzle. Notably, this technique can be performed utilizing less volatile liquids at room temperature. For example, Yang et al. [25] explored the feasibility of printing different viscosity silicones utilizing material jetting systems with dual piezoelectric/pneumatic mechanisms. The dual piezoelectric/pneumatic systems can produce sufficient force to jet pastes with viscosities up to 1,000,000 mPa·s under shear stress at the orifice. This newly proposed system enables the printing of silicone with a lateral resolution of 500–600 µm and a velocity of approximately 100 mm/s, which is 10–20 times faster than other direct write methods. In another case, Unkovskiy et al. [26] utilized drop-on-demand technology to manufacture a nasal prosthesis with a silicone free of solvents (ACEO Silicone General Purpose). The results indicated that wearing the prosthesis led to a reduction in follow-up appointments and an increase in aesthetic appearance compared to traditional methods.

### 2.1.3. Extrusion Processes

Highly accurate nozzle dispensing systems possess the ability to deposit a broad range of fluids, encompassing low viscous liquids and extremely thick pastes exhibiting viscosities as high as  $6 \times 10^7$  mPa·s (with a shear-thinning behavior), rendering them exceedingly well-suited to applications in additive manufacturing (AM). In contrast, the recommended maximum material viscosities for SLA and drop-on-demand inkjet printing processes fall within the ranges of 300–5000 mPa·s and 10–100 mPa·s, respectively. Utilization of diverse dispensing mechanisms enables the propulsion of fluids through a nozzle in material extrusion systems, with pneumatic and mechanical dispensing systems constituting the most commonly employed techniques. There are three types of silicone material extrusion processes: direct ink writing, complete support-embedded 3D printing and removable support-embedded 3D printing [27].

Direct ink writing refers to the printing material being stacked on the printing platform directly according to the scanning path through the extrusion nozzle. Ghazaleh et al. [28] used the Aerotech AGS1000 3D printing system with two independent z-axis heads to fabricate aortic root models. Four types of inks possessing distinct properties for the supporting material were employed and deposited utilizing four high-precision dispensers that controlled four dispensing apparatuses. The result showed that these models have the potential to open up new and compelling avenues for reducing the incidence of postoperative complications and aiding the advancement of cutting-edge medical devices. However, the viscosity of uncured silicone is low and not conducive to solidification and shaping in direct ink writing. To improve the solidification of liquid silicone, it is often self-supported by adding filler particles and other materials with stronger rheological properties, but this changes the material's mechanical properties (such as elastic modulus), making the printed products unable to meet design requirements. To avoid using filler particles, some researchers optimized direct inkjet printing technology and improved the nozzle squeezing method. Zhou et al. [29] proposed a universal 3D printing solution for silicone and PDMS soft materials, in which a real-time mixing printing nozzle was designed. The two-component silicone gel was stored separately and simultaneously extruded during printing and fully mixed with the help of mixing blades. The printable properties of silicone gel were improved by adding a rheological modifier (nano-silicon dioxide). Nano-silicon

dioxide particles dispersed in the silicone gel weakened the interaction between the silicone gel molecules, resulting in a significant increase in the viscosity of the material system.

Embedded 3D printing can be divided into complete support-embedded 3D printing and removable support-embedded 3D printing. In the process of support-embedded 3D printing, the complete supporting matrix is subjected to curing, whereas the printed inks may either be curable or non-curable. The support structure is first cured into the desired shape, and then the printing ink is extruded into the supporting structure. Christopher et al. [30] reviewed the sacrificial materials and related methods used for 3D printing of soft structures, including the use of sacrificial inks to print a temporary structure surrounded by permanent material, which is subsequently removed to create a hollow structure. Alternatively, permanent structures can be directly printed into sacrificial support materials, which act as a support matrix during the solidification or maturation process of the manufactured structure. The researchers established manufacturing principles for soft matter printing by analyzing literature data and explored printing performance within the context of instabilities controlled by the rheology of soft matter materials. So, supporting embedded printing is similar to a combination of casting and 3D printing. The external geometry of the final model is determined by the support structure, while the internal shape is determined by the printing ink [17].

Removable embedded printing refers to removing the cured printing ink model from the uncured support matrix. The curing process is different from that of the complete support method. In this process, the printing ink is cured, while the support matrix is not [31], as shown in Figure 3. The advantage of this technology is that it can print low-viscosity ultra-soft materials, but when printing solid fillings, the problem of the uncured support matrix being trapped during the printing process will occur. To solve this problem, Greenwood et al. [27] designed a supporting structure method based on movable embedded printing technology. The supporting structure only cures inside the printing ink structure and not in other positions within the reservoir. The results indicate that samples printed with this technology have an almost isotropic elastic modulus in the directions perpendicular and parallel to the printing layer, and the modulus is reduced at the fracture and the elongation rate increases compared with the removable support-embedded 3D printing. Furthermore, optimizing the design of support material can also improve molding efficiency. Duraive et al. [32] developed a support material made of silicone oil emulsion to weaken the interfacial tension of silicone-based ink. This support material eliminates the interfacial tension generated by the silicone gel ink during the printing process. Researchers used this technology to successfully print a silicone heart valve model, as shown in Figure 4.

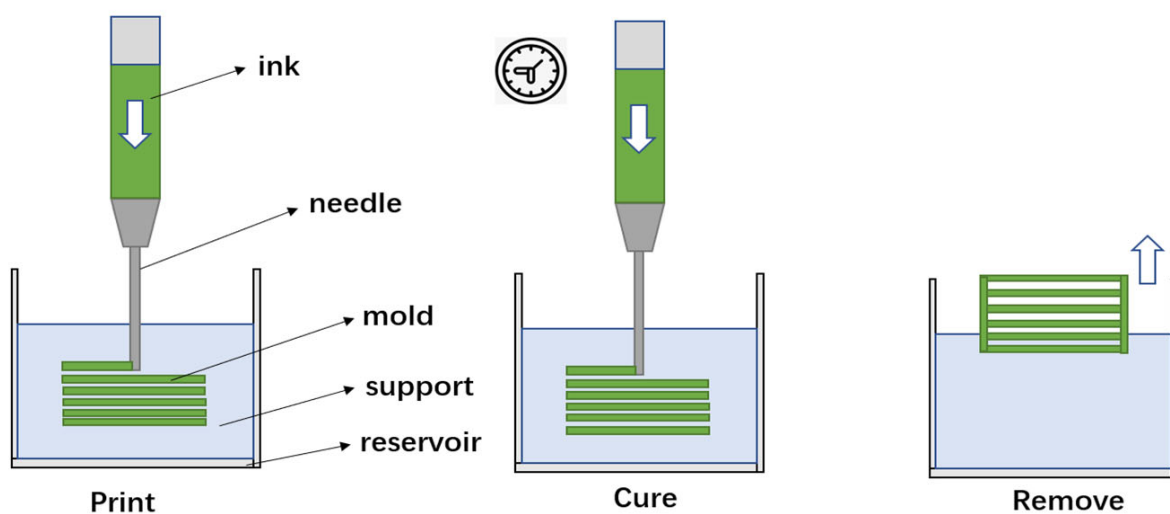
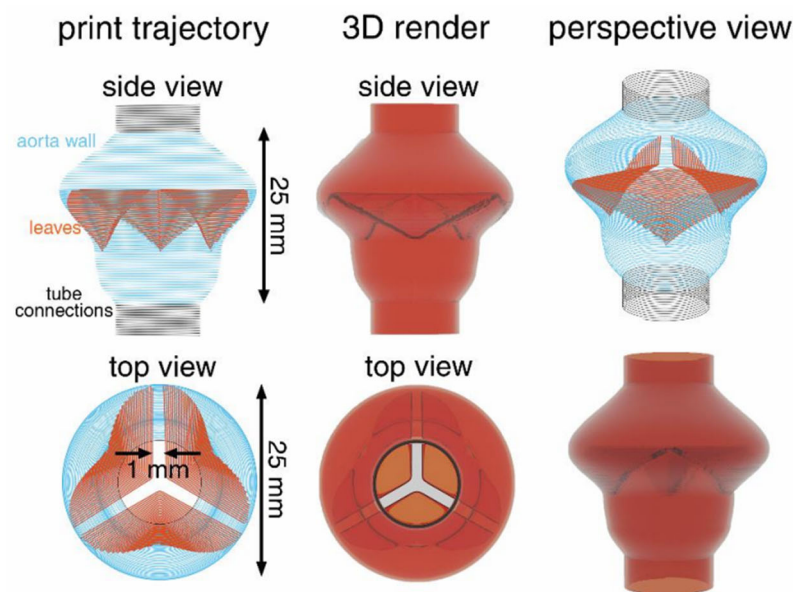


Figure 3. Removable support-embedded 3D printing.



**Figure 4.** Heart valve model.

## 2.2. Training and Surgical Planning

In the face of complex and difficult surgeries, such as digestive and cardiac valve surgeries, preoperative training and planning are essential for doctors to safely and efficiently complete these surgical procedures. In recent years, medical imaging technologies, such as CT and MRI, have seen rapid development, allowing medical personnel to accurately obtain three-dimensional data of patients' diseased areas. Using 3D printing technology, medical staff can quickly and accurately manufacture three-dimensional medical models of patients, providing doctors with a blueprint for preoperative planning and opportunities for repeated training.

Three-dimensionally printed medical models provide specific anatomical structures for doctors, avoiding spatial position misunderstandings caused by obtaining anatomical structures from CT, MRI, and other imaging techniques. Doctors can use the medical model for repeated practice, honing their surgical skills and reducing training costs. Corpse models have been the gold standard for surgical training, but they are extremely rare in major medical schools, which presents an opportunity for 3D-printed medical models to enter hospitals. Due to their personalized and precise characteristics, 3D-printed medical models have gradually become the standard model for preoperative training. Casas-Murillo et al. [33] designed a 3D-printed model for laparoscopic cholecystectomy using flexible materials. Thirteen surgeons evaluated the model and 61% of evaluators were satisfied with its realism, while 92% indicated that they would recommend it for training in laparoscopic cholecystectomy.

In digestive surgery, the digestive system has many complex and changing tubular channels, and doctors need to use endoscopic instruments to perform observations in narrow channels. Inexperienced young doctors cannot yet use endoscopic instruments skillfully and require accurate medical models to assist in their training and improve the accuracy of the surgery. Li et al. [34] divided 20 interns into a 3D-printed model training group and a virtual model training group, conducted 2 weeks of gallbladder anatomy learning and cholangioscopy technology training, and then evaluated the two groups' performance in cholangioscopy operation tests. The accuracy rate of the two groups in identifying bile duct anatomy was 95% and 27%, respectively, and the operation time of the 3D-printed model training group was shortened from  $29 \pm 8$  min before training to  $16 \pm 3$  min after training. Similarly, Zhang et al. [35] trained 16 surgeons with preliminary surgical experience in laparoscopic fundoplication using a structured evaluation tool to assess their performance. The 3D-printed model training group showed significant

improvement compared to the non-trained group, with shorter operation times. Preoperative training with 3D-printed medical models not only trains young doctors' skills, but also directly simulates actual surgical operations. As 3D-printed medical models can accurately simulate human tissue and organs, doctors can perform surgical rehearsals and become familiar with surgical operations. This means that before performing actual surgery, doctors have already undergone a lot of practice and surgery, greatly improving the accuracy and efficiency of the surgery. Wei et al. [36] successfully constructed a 3D-printed surgical model for the minimally invasive radical resection of extrahepatic bile duct cancer, simulating blood and bile circulation in the portal vein and bile duct, and invited six hepatobiliary surgeons to perform laparoscopic or robotic surgeries, all of which were completed successfully.

In terms of valvular heart disease, 3D-printed medical models can display the anatomical location of lesions and adjacent relationships with surrounding organs and blood vessels in a three-dimensional, clear, and specific manner, which roughly corresponds to the actual situation during surgery. Therefore, 3D-printed medical models can help doctors to understand the anatomical characteristics of the affected area and provide a reference blueprint for clinical decision-making and surgical planning. Engelhardt et al. [37] constructed a three-dimensional structure of the mitral valve for patients with severe mitral regurgitation based on transesophageal echocardiography and computed tomography. They used 3D printing technology to create a high-fidelity silicone model of the mitral valve and performed preoperative simulated repairs. By simulating the surgery on the 3D model before the operation, they devised the best surgical plan, and the operation proceeded smoothly. Imbrie et al. [38] demonstrated a 3D-printed valve dilator device that accurately simulates various degrees of mitral regurgitation induced by annular dilation. This device was used to design and optimize surgical repair plans through *in vitro* experiments. In addition to this, personalized medical strategies using 3D printing not only make complex surgeries repeatable but also improve patient safety and the effectiveness of treatment. Zelis et al. [39] created a model of a narrowed aortic valve using 3D printing technology. They achieved good surgical results through preoperative evaluation, simulation, intraoperative guidance, and postoperative evaluations.

### 3. Surgical Navigation Template

Computer-assisted navigation technology utilizes computers and medical robots for surgical intervention, allowing the real-time display of position during surgery. However, this technology has made the surgical procedure more complex, lengthening operation time and increasing surgical difficulty. Additionally, computer-assisted navigation equipment is expensive, and the navigation system is unstable, making clinical application difficult. Three-dimensionally printed surgical navigation templates, based on human biological data, can fit the patient's surgical site and guide the surgery along pre-determined trajectories. Interactive surgical navigation templates can reduce the cost of surgical navigation, simplify surgical procedures, and increase surgical precision compared to computer-assisted navigation systems. Currently, 3D-printed surgical navigation templates are widely used in surgical assistive fixation for knee joints, spine, hip joints, and surgical trauma. Based on the clinical use of 3D-printed orthopedic surgical guides, templates can be divided into nail-plate guides, osteotomy guides, and other series of guides.

#### 3.1. Osteotomy Guide Plate

Traditional osteotomy surgeries often use the X-ray plotting method, making it difficult to effectively execute the angle of osteotomy during surgery. In traditional joint replacement surgeries, doctors mainly rely on preoperative imaging data and intraoperative osteotomy guides to determine the amount and scope of osteotomy, while accurate osteotomy and perfect reconstruction of the lower limb axis is the key to achieving excellent postoperative outcomes [40]. Therefore, precise osteotomy during surgery is very challenging and has a significant negative impact on surgical outcomes.

Osteotomy guides are mainly used to guide the location, depth, and direction of osteotomy, thereby improving the accuracy of force line correction, the fitting between prostheses or implants and the affected area, and can effectively quantify preoperative planning, thus improving the accuracy of osteotomy and reducing the difficulty of surgery [41–43]. Three-dimensionally printed guides have been applied successfully in osteotomy surgeries. The patient’s imaging data are processed using digital software to reconstruct the model of the patient’s affected area and prosthesis. Based on this, a matching osteotomy guide is designed for the patient’s surgical site to improve surgical accuracy. Hafez et al. [44] conducted experimental research on cadaveric specimens, and for the first time, used knee joint CT data to create individualized osteotomy templates for use in TKA surgery. Compared with previous methods, the template operation was simpler, less invasive, and time-saving. Ikram et al. [45] used 3D printing technology for TKA surgery and compared the predicted amount of osteotomy before surgery with the actual amount of osteotomy during surgery. The results showed that 90% of the osteotomy errors were <1 mm, and there were no complications or infections in any of the TKA surgeries. Jie Yu et al. [46] analyzed the efficacy of 3D-printed navigation templates in Salter osteotomy for children with DDH. The researchers evaluated 32 consecutive patients who underwent Salter osteotomy and divided them into a conventional group (n = 16) and a navigation template group (n = 16) according to different surgical methods. The two groups were compared in terms of acetabular correction, radiation exposure, and surgical time, as shown in Figure 5. The results showed that compared with the conventional group, the navigation template group had more accurate acetabular correction, less radiation exposure, and shorter surgical time. At the same time, the navigation template group achieved better surgical outcomes than the conventional group.

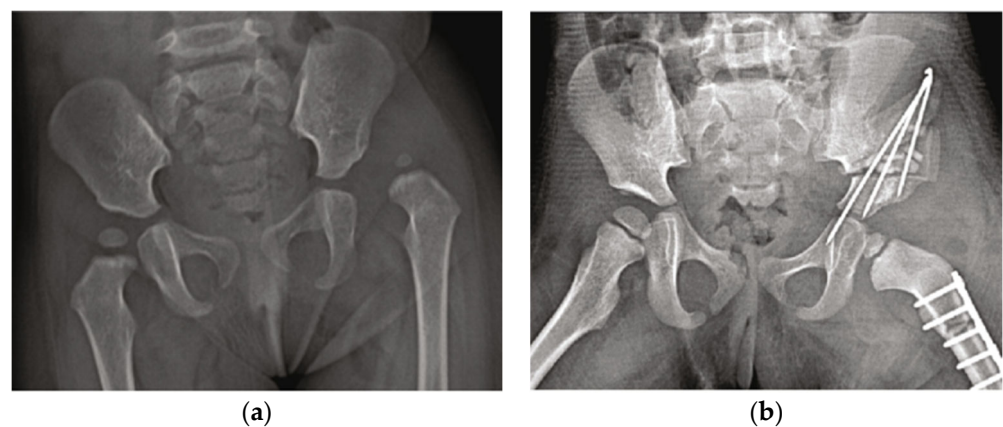


**Figure 5.** This picture is cited from “Accuracy of Bone Resection in Total Knee Arthroplasty using CT Assisted-3D Printed Patient Specific Cutting Guides” [46]. This picture shows the effect of the surgical navigation template. (a) Anteroposterior X-ray of the pelvis before surgery. (b) Anteroposterior X-ray of the pelvis after surgery.

### 3.2. Guide Plate for Nail Placement

The guide plate for nail placement is used to guide the position and angle of nail placement in orthopedic surgery to improve the safety and accuracy of nail placement [47]. For example, the spinal and pelvic areas are adjacent to important blood vessels and nerves with complex anatomical structures. Deviations in the position and angle of screw placement during surgery can affect adjacent spinal cords and nerves, and lead to a significant decrease in fixation strength, and, in severe cases, can cause vertebral artery injury [48,49]. When patients also have spinal deformities, the difficulty of accurately placing pedicle screws is further increased [50]. Using 3D-printed navigation templates to determine the position and direction of nail placement can improve the accuracy of pedicle screw placement in surgery [51]. The workflow mainly includes first reconstructing a 3D vertebral

model based on CT scan data and using it to design a navigation template consistent with its anatomical structure, and then integrating the optimal screw trajectory with the navigation template to design a navigation template with guide holes.

Sugawara et al. [52] applied 3D navigation template technology to clinical practice and inserted 58 pedicle screws using 3D-printed templates in 10 patients with thoracic and cervicothoracic vertebral lesions. Postoperative CT images showed that the screws did not penetrate the pedicle cortex, and the average deviation from the expected screw trajectory at the coronal midpoint of the pedicle was  $0.87 \pm 0.34$  mm, indicating that the screw placement was very successful. Liang et al. [53] analyzed the practicality of navigation templates in guiding accurate placement of iliac screws. The researchers collected preoperative CT images of eight patients with pelvic fractures to reconstruct a 3D pelvic model, and designed and printed a surgical navigation template for the position of the iliac screw based on this model. The researchers used the surgical navigation template for intraoperative deep screw positioning on the iliac crest, and according to postoperative X-rays and CT scans, there were no significant differences in the entry point, convergence angle, and tail angle of the screw before and after surgery. The results showed that personalized surgical navigation templates are an improvement over traditional techniques, can improve positioning accuracy and depth, and have good mechanical stability and lower risk of screw-related complications. Wenjie Shi et al. [54] improved the placement of cortical bone trajectory screws in the lumbar spine using a navigation template. They reconstructed a 3D lumbar spine bone model based on CT scan data and made a surgical navigation template from it. The researchers used the same surgical navigation template to insert cortical trajectory screws into both 3D-printed navigation templates and cadaveric specimens. After screw insertion, they directly observed the screw path in the 3D-printed specimen and determined the screw position and direction by CT scanning the anatomical specimen. The results showed that the excellent rate of screw placement was 100% and 95% in each 3D-printed specimen and anatomical specimen, respectively.

The use of digital technology to reconstruct patient-specific disease models, combined with 3D printing technology to manufacture surgical navigation templates, can effectively guide surgeons in the placement of internal fixation devices, the repositioning of bones, and the determination of bone cutting ranges. However, the research on 3D-printed surgical navigation templates has mainly focused on clinical applications, with less attention paid to the design methods, formative accuracy, and performance evaluation of the templates. Additionally, during surgery, navigation templates may require the removal of more soft tissue to better match the anatomical structure and avoid interference from soft tissue. Nevertheless, the question of whether the implantation of navigation templates needs to consider soft tissue remains controversial. Currently, personalized 3D-printed surgical navigation templates have become more mature, but there are still few long-term research cases, and the quality of navigation templates lacks unified standards, requiring considerable clinical data on 3D-printed navigation template applications. Therefore, further research on the development and application of 3D-printed personalized surgical navigation templates is necessary.

#### 4. Invisible Aligners

Most of the invisible aligners currently used in the market are produced by using 3D-printed dental models as the mother molds, and then applying thermoforming technology to attach medical films to the resin mother molds for compression molding. However, this method produces aligners with uncontrollable thickness throughout the entire structure, making it impossible to estimate the generated force during the correction process, which may affect the final correction result by affecting tooth posture changes [55]. With the development of new materials and 3D printing technology, there has been growing interest in combining invisible orthodontic aligners with 3D printing technology [56–58]. Direct 3D printing technology allows for personalized customization according to patients' specific conditions, making the aligners adaptable to the complex and multi-curved surface shapes

of teeth in the oral cavity, and can simplify the thermoforming steps, ultimately achieving personalized diagnosis, treatment, and precision medicine in the clinic [59]. Currently, the main 3D printing technologies that can be applied to the manufacture of invisible aligners are SLA technology, SLS technology, and FDM technology, and the workflow of directly 3D printing invisible aligners is shown in Figure 6. Among these, photosensitive resin material has the advantages of strong fluidity, fast photocuring speed, and high manufacturing precision, making it the optimal choice for printing invisible aligners [60].

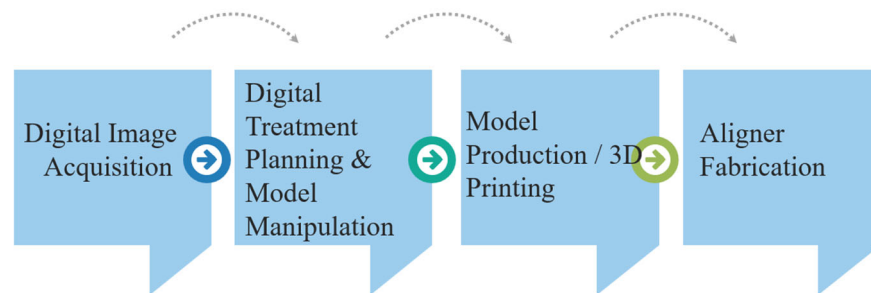


**Figure 6.** Workflow of the direct 3D printing of invisible aligners.

The accuracy of three-dimensional (3D) model reconstruction plays a crucial role in determining the quality of the final parts produced by the entire 3D printing technology process. In practice, achieving higher product formation accuracy for specific materials and 3D printing processes hinges on a critical step before printing: the reconstruction of a precise 3D virtual model. In the field of oral aesthetic restoration, computer-aided design and computer-aided manufacturing (CAD/CAM) technology has demonstrated sufficient reliability. By using computed tomography (CT) scanning or magnetic resonance imaging (MRI) techniques to obtain the anatomic structure features of patients and then leveraging CAD/CAM technology, precision 3D model reconstruction can be effectively achieved. For example, the surface-to-surface matching technique allows the superimposition of 3D objects to evaluate the Euclidean distances between the relative surfaces; also, this digital technique provides, on a 3D color map, the morphological differences between the superimposed structures in different colors by setting specific levels of tolerance, as shown in Figure 7. Achieving precise segmentation is crucial for the physical reconstruction of anatomy, specifically in the context of 3D printing, in order to minimize errors and ensure accuracy. Lo Giudice et al. [61] assessed the precision of four distinct software programs in the semiautomatic segmentation of the mandibular jaw, in comparison with the manual segmentation approach that is considered as a gold standard. Twenty cone beam computed tomography (CBCT) scans were selected to compare the efficiency of manual segmentation using Mimics software versus four different semi-automatic approaches—Invesalious, ITK-Snap, Dolphin 3D, and Slicer 3D—for mandible segmentation. The results show that there were no significant differences observed in the overall volume in 3D mandible models. However, different software produced varying matching percentages for the generated mandible models, and there was a high correlation between semi-automatic and manual segmentation methods. Similarly, Lo Giudice et al. [62] assessed the accuracy of mock-ups produced through the use of milling and 3D printing technology in combination with a full digital workflow system. Ten adult subjects were selected, and digital analysis of the trueness was carried out by means of surface matching of scanned-milled models and scanned-prototype models with digital waxing. Specific linear measurements were also taken. The results showed that the prototype models exhibited a significant increase in horizontal measurements, whereas the milled models showed a significant increase in both vertical and horizontal measurements. Notably, the prototype models demonstrated better fit performance. It can be seen that the study by Lo Giudice et al. has some instructional significance for improving the accuracy of 3D model reconstruction.

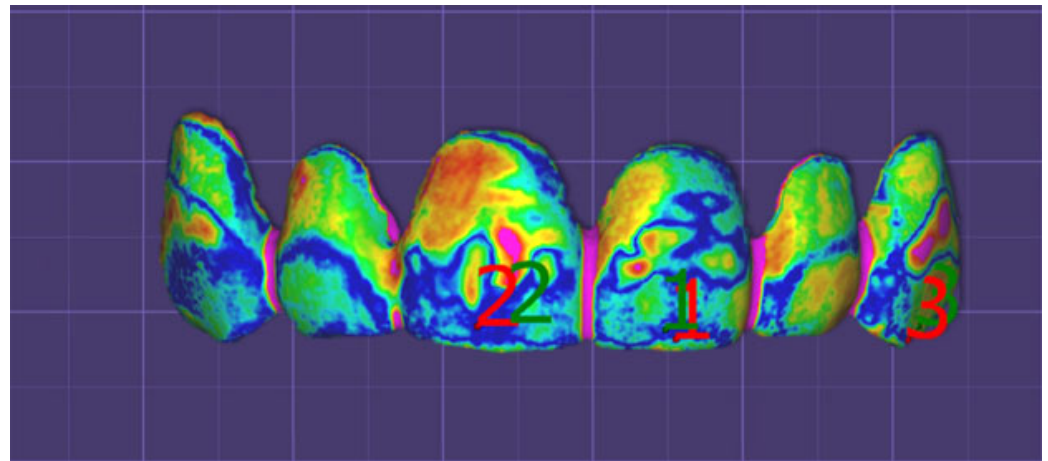


**Figure 7.** This picture is cited from “The step further smile virtual planning: Milled versus Prototyped Mock-Ups for the Evaluation of the Designed Smile Characteristics” [62]. This picture shows the color-coded map according to the surface-to-surface analysis.

To be used for invisible orthodontic aligners, the material needs to meet certain conditions, including non-toxicity to cells, biocompatibility, and suitability for 3D printing processes. Dental LT resin was the first material used for the direct 3D printing of invisible aligners. Compared to traditional thermoplastic molding techniques, using this material for photocuring molding produces aligners with higher precision and greater comfort for patients. Another material that can be used for direct 3D printing is TC-85, a photosensitive resin material with high flexibility, low viscosity, and aligners that exert less pressure on teeth while maintaining continuous correction force. In addition, the material’s high-temperature stability and shape memory properties provide it with advantages in clinical applications. Currently, there are no certified transparent materials available on the market for the direct 3D printing of invisible aligners.

To investigate the feasibility of directly 3D printing invisible aligners, some researchers compared the mechanical properties and geometric accuracy between direct 3D printing and hot-press molded aligners. In 2014, Nasef et al. [63] first attempted to use direct 3D printing to produce dental fixators, but did not evaluate their accuracy. Subsequently, Jindal et al. [64] directly 3D printed 0.75 mm LT orthodontic aligners and compared them with thermoformed Duran aligners. The results showed that the geometric accuracy of the 3D-printed cured aligners was more accurate than thermoforming, which can cause plastic and irreversible deformation, resulting in large displacement, while the deformation of 3D printing has the elasticity of reversibility for lower displacement. However, this study lacked clinical data to evaluate the effect of Dental LT resin and its durability.

The 3D printing process has a significant impact on its printing quality, and when direct 3D printing invisible aligners, factors such as the printing equipment, ambient temperature, curing time, etc., need to be considered. Some researchers analyzed the factors that affect the direct 3D printing of aligners. Zinelis et al. [65] compared the mechanical properties of invisible aligners produced by different printing equipment, selecting TC-85DAW to be printed using five different printing devices, and the results showed that the orthodontic aligner was different in terms of Martens hardness, indentation modulus, elastic index, etc., under different conditions. In addition, the 3D-printed model’s orientation and curing time may also affect the performance of the product. McCarty et al. [66] investigated the impact of model printing direction and curing time on the mechanical properties. They designed different printing angles such as horizontal, vertical, and 45°, and compared them with different photosensitive curing times. The results showed that they had little effect on the overall dimensions. Relevant studies have also shown that improving the mechanical isotropy of the model can improve its mechanical properties compared to improving the accuracy of the invisible aligner [67]. However, when using 3D printing to

produce invisible orthodontic aligners, its design thickness cannot be accurately controlled. Moreover, controlling its printing thickness is more complex, and the effect is not ideal.

## 5. Implants

### 5.1. PEEK Implants

Polyetheretherketone (PEEK) is a semi-crystalline polymer material with excellent mechanical properties, good biocompatibility, and X-ray transparency. In particular, PEEK has an elastic modulus that is closer to normal human bone tissue, thereby reducing or eliminating stress shielding effects. However, pure PEEK is a biologically inert material that is not conducive to the adhesion and proliferation of osteoblasts, resulting in poor osseointegration and limited application in bone implants [68]. Incorporating active particles or fiber-reinforced materials into PEEK can effectively enhance its biological activity and improve its binding efficiency with bone tissue. Such composite materials mainly include hydroxyapatite–PEEK composites optimized for bone activity and carbon fiber-reinforced PEEK composites optimized for mechanical properties [69]. Han et al. [70] used FDM technology to print pure PEEK and carbon fiber-reinforced PEEK composite materials, and the results showed that the mechanical strength of CFR-PEEK samples after 3D printing was significantly better than that of pure PEEK specimens.

The 3D printing technologies for PEEK and its composite materials mainly include selective laser sintering (SLS) and fused deposition modeling (FDM). SLS printing technology has high accuracy and can print complex lattice or hollow structures, but most SLS devices cannot perform multi-material printing, making them unsuitable for printing PEEK composites [71]. The FDM printing process uses filament printing, where the material is melted and extruded through a nozzle and deposited layer by layer on the work platform along the scanning path to form the object [72]. Using the FDM process to print PEEK composite models, filaments of hydroxyapatite–PEEK and carbon fiber-reinforced PEEK composites can be prepared in advance and then printed using FDM equipment, making it suitable for the 3D printing of complex-shaped composite bone implants.

The mechanical properties of PEEK composite products produced using FDM printing are influenced by various factors, primarily the printing parameters and materials used. Different PEEK composite materials result in products with different mechanical properties, with an important influencing factor being the material ratio. Oladapo et al. [73] demonstrated that for hydroxyapatite–PEEK composites, the quality fraction of hydroxyapatite is generally between 0% and 20%, with PEEK/CHAP composites containing 15% exhibiting optimal mechanical properties. For CF/PEEK and GF/PEEK composites, Wang et al. [74] found that 5% CF/PEEK and 5% GF/PEEK exhibit higher tensile and flexural strengths.

In addition to considering the mechanical properties of PEEK composite materials, biocompatibility with bone tissue must also be taken into account, whereby implants must have good adhesion, osteoconductivity, and cell activity to fuse well with bone tissue. The combination of HA and PEEK can significantly improve the osteogenic activity of cells and enhance the bioactivity of PEEK. Zheng et al. [75] demonstrated that PEEK–HA composite scaffolds produced using FDM can promote MC3T3-E1 cell adhesion and mineralization due to their porous surface structure. Considering the good mechanical properties of PEEK materials, new approaches have been proposed for the treatment of jawbone defects. For instance, Mohamed et al. [76] used a 3D-printed PEEK mesh to fix severely damaged alveolar bone, which was found to increase bone volume. Similarly, Kang et al. [77] utilized 3D-printed PEEK implants to fix the fibula and restore the continuity of the mandible, resulting in improved safety and stability. Moreover, 3D-printed PEEK composite dentures exhibit significant advantages in retention force, stability, and comfort. Chen et al. [78] fabricated denture bases using a TiO<sub>2</sub>- and PEEK-based PMMA composite resin using 3D printing technology, and the experimental results demonstrated ideal mechanical properties and antibacterial activity.

In summary, producing PEEK composite products using FDM printing involves optimizing material ratios and printing parameters to achieve optimal mechanical properties.

Biocompatibility with bone tissue is also critical, and adding HA to PEEK can enhance its bioactivity. PEEK is a promising material for repairing jawbone defects, and 3D-printed PEEK composite dentures exhibit significant advantages in terms of retention force, stability, and comfort.

### 5.2. Titanium Alloy Implants

In the field of 3D printing of metal implants, porous metallic materials are the preferred choice for orthopedic hard implants, with Ti-6Al-4V being the most important material due to its superior mechanical properties and biocompatibility with tissues [79]. Compared to stainless steel and other metals, titanium has a more favorable strength-to-weight ratio and a smaller modulus of elasticity, enabling medical titanium alloys to exhibit better performance, particularly in terms of the ability to promote bone tissue growth and fusion into the implant. Laser-based 3D printing techniques such as selective laser melting (SLM) are highly promising solutions for this field. Researchers have conducted studies on the SLM printing process of Ti-6Al-4V, aiming to obtain Ti6Al4V implants with high density, low roughness, and excellent mechanical properties. Edwards et al. [80] investigated the effect of different stacking orientations on the fracture toughness and fatigue crack growth behavior of Ti6Al4V specimens produced by SLM process. It was found that the average results of crack propagation in three directions and the critical stress intensity values did not differ significantly. L.Y. Chen et al. [81] investigated the anisotropic response of hardness and electrochemical behavior of Ti6Al4V specimens prepared by means of SLM using a zigzag laser scanning path in the X, Y, and Z directions. It was found that the hardness was approximately 20% lower in the cross-sectional direction perpendicular to the laser motion compared to the other two directions, and the corrosion resistance was the lowest.

The clinical application of 3D-printed metal implants has gradually developed. Titanium alloy implants manufactured using electron beam selective melting (EBSM) technology obtained European CE and US FDA certification in 2007 and 2010, respectively. Three-dimensional printing technology can print personalized metal implants for human repair and reconstruction. Dekker et al. [82] treated 15 patients with complex large bone defects and deformities using custom 3D-printed titanium alloy scaffolds. After 22 months of follow-up, CT image fusion occurred in 13 cases, and pain was significantly improved. Mobbs et al. [83] used laser direct melting technology (similar to LENS technology) to manufacture patient-specific custom anterior lumbar interbody fusion (ALIF) implants and successfully performed anterior lumbar interbody fusion surgery, significantly shortening the operation time. Belvedere et al. [84] designed and customized three CoCrMo ankle joints using SLM technology, and successfully performed replacement surgery, achieving good results in joint mobility and stability after surgery. Xu et al. [85] reported the use of 3D-printed personalized titanium alloy prostheses to treat bone defects after pelvic tumor resection. Through preoperative computer-aided design, combined use of 3D-printed tumor resection guides, prosthesis installation guides, and personalized 3D-printed titanium alloy prostheses for repair and reconstruction after pelvic tumor resection, more accurate tumor resection and more ideal prosthesis shape and mechanical matching can be achieved, reducing surgical trauma, shortening operation time, and promoting postoperative functional recovery.

Titanium alloy implants are able to meet the requirements of repairing and reconstructing human tissue, but they need to maintain a certain level of strength, hardness, and elasticity within the human body to support functions such as weight bearing [86]. To ensure that metal implants can effectively transfer loads to adjacent bone tissues and avoid relative displacement between the implant and bone, the structure of the implant can be optimized. The structure of titanium alloy implants has a significant impact on their mechanical properties, with the pore structure and porosity having a direct effect on the mechanical performance of porous bodies, as well as the biomechanical compatibility of porous implants in the human body. Jian Li et al. [87] studied the mechanical properties of porous implants with diamond, rhombic dodecahedron (RD), and octahedral truss (OT)

pore structures, as shown in Figure 8. The results showed that different pore structure units can directly affect the mechanical properties of porous implants and provide different biomechanical behaviors. The rhombic dodecahedron pore structure has better comprehensive mechanical properties. The RD and OT pore structures with central symmetry have better compression performance than the DO pore structure with diagonal symmetry. The elastic modulus of the Ti6Al4V porous body samples with three pore structures printed using 3D printing is between 2.59 and 4.89 GPa, which is similar to the mechanical properties of human bones.

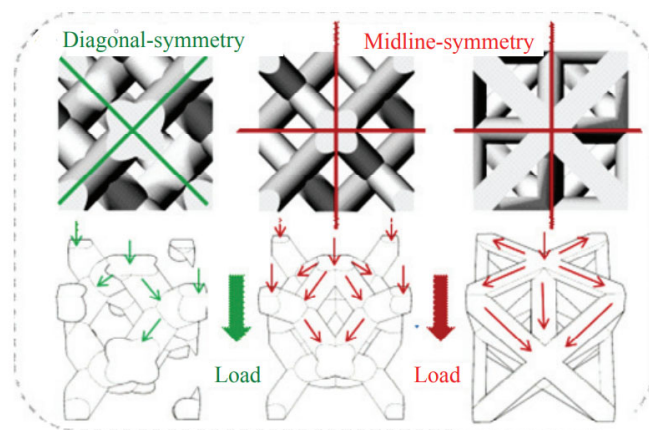


**Figure 8.** DO, RD and OT shape. This picture is cited from “Diagonal-Symmetrical and Midline-Symmetrical Unit Cells with Same Porosity for Bone Implant: Mechanical Properties Evaluation” [87].

In another study, Epasto et al. [88] specifically studied the static and dynamic mechanical properties of 3D-printed rhombic dodecahedron porous Ti6Al4V samples and discussed the influence of unit size and pillar diameter on mechanical properties. The experimental results reached a similar conclusion that the rhombic dodecahedron structure has good compressive strength and a low elastic modulus, and is a suitable solution for low-stiffness applications such as biomedical implants. Similarly, changes in pore size also affect the performance of the implant, and uniform pore size and non-uniform pore size have different effects.

Wang et al. [89] used an improved non-uniform pore size porous design and electron beam melting (EBM) technology to prepare a Ti-6Al-4V titanium alloy structure, and from the perspective of mechanical properties and biological reactions, the non-uniform pore size porous design has an acceptable Young’s modulus and compressive strength values, showing mechanical properties similar to bone, with a Young’s modulus of 8–15 GPa and strength of 150–250 MPa. As can be seen, the clinical application of 3D-printed metal implants is still mainly based on printing titanium alloy materials. Although titanium alloy materials have good performance, there are still some pressing issues that need to be addressed: although Ti-6Al-4V materials with porous structures have good comprehensive physicochemical properties, there is still a “stress shielding” phenomenon, which increases the possibility of reducing bone healing rates. Furthermore, there are currently few systematic biological evaluations and effectiveness studies on porous titanium alloys, as well as verifications of post-processing effects after the 3D printing of porous titanium alloys.

In addition to implantable materials, there are other biological materials that can be used for human implants. Generally speaking, clinical medicine has the following basic requirements for biomedical materials: (1) non-toxic, non-carcinogenic, non-teratogenic, and do not cause sudden reactions of human cells or tissue cell reactions; (2) good compatibility with human tissues, do not cause poisoning, hemolysis, coagulation, fever, and allergic reactions; (3) stable chemical properties, resistant to the action of antibodies, blood, and enzymes; (4) have physical and mechanical properties that are compatible with natural

tissues; and (5) have specific functions for different application purposes. More implant materials are discussed for comparison in Table 3.

**Table 3.** The characteristics and applications of different implant materials.

Materials	Characteristics	3D Technology	Applications
Co-Cr Alloy	Strong corrosion resistance, high hardness, excellent mechanical properties, and low cost	Selective laser melting Electron beam selective melting	Prosthesis, fixation screw, bone plate, denture, cobalt-chromium alloy porcelain-fused-to-metal crown
316L Stainless Steel	Excellent mechanical properties, favorable biocompatibility, good corrosion resistance, and low cost	Selective laser melting Electron beam selective melting	Fracture internal fixation, cardiovascular intervention therapy, dental implant and periodontitis treatment stent
Tantalum	Corrosion resistance, good plasticity, excellent biocompatibility	Selective laser melting Electron beam selective melting	Spinal fusion surgery, cranial shaping surgery, ankle surgery, tumor reconstruction surgery
Titanium Alloy	Low material density, low elastic modulus, good mechanical properties, corrosion resistance, biocompatibility	Selective laser melting Electron beam selective melting	Joint replacement surgery, percutaneous coronary intervention (PCI), dental implantation, periodontal scaffold
Magnesium Alloy	Similar to bone density, enhances osteoblast proliferation, promotes bone growth and healing	Selective laser melting Electron beam selective melting	Biodegradable cardiovascular stent, bone plate, fixed screw
PLA	Biocompatible and biodegradable	Fused deposition modeling Selective laser sintering	Soft tissue repair, bone repair
PMMA	Good plasticity, stable chemical structure, and good mechanical properties	Fused deposition modeling Selective laser sintering	Fracture repair, joint replacement surgery, spinal surgery, denture, dental crown restoration, cochlear implants
PEEK	Good biocompatibility and chemical stability, elastic modulus similar to human bone	Fused deposition modeling Selective laser sintering	Spinal fusion device, artificial intervertebral disc, bone plate, tissue scaffold
Hydrogel	Good hydrophilicity, biocompatibility, and biodegradability	Stereolithography Embedded 3D printing Material jetting	Tissue scaffold, heart valve, vascular and dermal tissue, drug delivery

## 6. Discussion and Prospects

As an advanced manufacturing technology, 3D printing technology combined with personalized precision medicine has brought about new breakthroughs in the medical field. Currently, there are various types of 3D printing technologies that can be applied in the medical field, including FDM, SLA, SLS, SLM, and silicon printing technology. Materials that can be used include plastic materials, metal materials, composite materials, and flexible materials. It can be seen that 3D printing technology has significant advantages in the application of precision medicine.

Firstly, it can improve material utilization and save materials. Traditional metal processing produces a surprisingly high amount of material waste, and some fine production processes can even result in the discarding of 90% of raw materials. However, the waste generated by 3D printers will be significantly reduced, and as printing materials continue to improve, 3D-printed “net-shaping” manufacturing will become a more environmentally friendly way of processing.

Secondly, 3D printing technology can achieve integration molding. The 3D printing process no longer requires traditional tools, fixtures, machine tools, or any molds. In modern factories, machines produce identical parts, which are then assembled by workers. The more components a product has, the more time and cost it takes to assemble. However, the feature of 3D printing’s integrated molding eliminates the need for further assembly, thereby shortening product delivery times.

Furthermore, 3D printing technology can achieve diversified production without increasing costs. With regard to traditional manufacturing, the more complex the shape of an object, the higher the manufacturing cost. However, for 3D printers, the cost of producing complex-shaped objects does not correspondingly increase. In addition, traditional manufacturing equipment has limited functions, resulting in limited types of shaped items being produced. One 3D printer can print different shapes, and like a craftsman, it can make differently shaped objects every time. This kind of manufacturing diversification

without increasing costs will fundamentally break the traditional pricing model and change the cost composition of our entire manufacturing industry.

Finally, 3D printing technology can achieve multi-material manufacturing molding. Traditional manufacturing machines find it difficult to merge multiple raw materials during cutting or mold forming processes, but 3D printing allows for the arbitrary combination of raw materials, enabling the creation of performance structures that people desire. For example, nylon-glass fiber or nylon-carbon fiber composite materials can improve the mechanical properties of nylon, and adding 50% titanium metal to nickel alloy powder can significantly improve its performance. For example, nylon-glass fiber or nylon-carbon fiber composite materials can improve the mechanical properties of nylon, and adding 50% titanium metal to nickel alloy powder can significantly improve its performance.

Based on the aforementioned technological advantages, 3D printing technology can rapidly and accurately manufacture complex medical assistive devices that conform to human characteristics. This will greatly improve the efficiency of precision medicine. Three-dimensionally printed personalized medical auxiliary devices have gradually entered clinical applications and serve as an important connection point between new medical engineering and clinical practice, showing promising application prospects and development trends. However, there are still some deficiencies in the current applications of 3D-printed auxiliary devices, mainly in the following areas related to medical applications discussed in this paper:

- (1) Strength issue: Compared with traditional manufacturing, products manufactured by means of 3D printing have certain differences in many aspects such as strength, hardness, and flexibility. The manufacturing process of 3D printing is additive, layer-by-layer production, which makes it difficult to match the material properties achieved by traditional molding techniques, even if the layers are bonded tightly. Currently, 3D-printed products cannot be used on a large scale as functional parts.
- (2) Accuracy issue: Due to the layer-by-layer production method of 3D printing, there is a common “stair-step effect”, especially when manufacturing objects with curved surfaces, which inevitably leads to deviations in accuracy. In addition, many 3D-printed objects require secondary processing such as sanding and high-temperature heating. The produced objects can easily warp due to material shrinkage, further reducing their accuracy.
- (3) It is difficult to achieve functional medical models. Although 3D-printed personalized medical models can solve the problem of the scarcity and high cost of medical training models, and provide medical staff with a three-dimensional understanding of patients’ anatomical structures, these models are still static. Currently, silicone medical models can simulate the flexibility of human organs, but lack functional simulation, which means that 3D-printed models cannot truly simulate the physiological characteristics of the human body. In complex minimally invasive surgeries such as those involving the heart, major blood vessels, and neurovasculature, functional medical models will provide precise surgical guidance to medical personnel, thereby achieving high-precision medical outcomes.
- (4) It is difficult to establish uniform quality testing standards. Surgical navigation templates, invisible orthodontic appliances, and human implants can all be considered medical auxiliary devices. Due to the differentiated physiological characteristics of the human body, medical devices manufactured through 3D printing are personalized rather than standardized. Establishing quality assessment standards for these personalized auxiliary devices is therefore challenging. Without quality testing standards, it will be difficult to determine the performance of these devices, increasing clinical application costs and reducing medical efficacy. This deficiency will also severely hinder the application and promotion of 3D printing technology in the market.
- (5) Static auxiliary devices cannot adapt to complex biomechanical characteristics. Invisible orthodontic appliances need to move with the upper and lower jawbones and be subject to dynamic tooth forces, while implants in the human body need to

be in contact with bone tissue and withstand certain stresses. Three-dimensionally printed internal auxiliary devices in the human body will experience complex and variable stress conditions, but the devices cannot change with changing surrounding conditions. This lack of dynamic biological characteristics makes it difficult for these auxiliary devices to adapt to complex human tissue structures, thereby reducing their therapeutic effectiveness.

In order to promote the widespread application of 3D printing technology in clinical settings, future research on precise medical applications of 3D printing can be developed through the following areas, based on the current research of 3D printing medical applications:

- (1) Developing application standards for 3D printing medical auxiliary devices. The major obstacle for promoting the application of 3D printing medical devices is the lack of corresponding quality testing standards. Traditional inspection standards for manufactured parts are relatively straightforward to develop, as common indicators can be summarized for mass-produced parts. However, 3D printing medical devices are personalized and their application cases are also individualized, making it difficult to find uniform quality testing standards to evaluate their printing quality and clinical effectiveness. In order to establish a sound set of quality testing standards for 3D printing medical devices, application standards for 3D printing can be added to existing standards, such as material standards and surface quality standards.
- (2) Conducting applications of 4D printing technology. The human body can be understood as a complex and variable biological field, making it difficult for static and unchanging internal assistive devices to adapt to this dynamic environment. Research and development of assistive devices that can adapt to changes in working conditions can greatly improve medical effectiveness. These devices can respond to changes in the surrounding physical field, and their structure also correspondingly changes to meet the compatibility with other tissues and avoid the impact of biologic forces. Four-dimensional printing technology can achieve the effect of corresponding structural changes due to changes in temperature, humidity, and mechanics, etc., and has good adaptability in the human body. For example, an invisible orthodontic appliance manufactured using 4D printing technology can adapt to new mechanical conditions as the force field between the appliance and teeth changes due to changes in biting or alignment. However, controlling its structure is still a challenge that requires extensive research.
- (3) Development of new materials and new processes. Biocompatibility is an important performance of internal assistive devices. Traditional single implant materials cannot meet the biological characteristics of human tissues, including biomechanical properties and biocompatibility. The clinical demand for implants with excellent biocompatibility will greatly increase. The development of new composite materials and their printing processes can improve the level of medical treatment and enhance the effectiveness of precision medicine. This is an important research direction for 3D printing of human implants. For example, tantalum metal has excellent biocompatibility and has become a research hotspot for orthopedic implants. However, the clinical application of 3D-printed porous tantalum is limited, and there is a lack of supporting design theories and manufacturing processes. Related studies are not yet systematic. Therefore, research on new materials, composite materials and their 3D printing processes is an important breakthrough for achieving precise 3D printing of medical implants.
- (4) Intelligent manufacturing applications. Traditional 3D printing of medical models cannot record information such as the force, position, and motion trajectory of the operator's actions, and the level of skill and training effectiveness cannot be quantified. By combining multi-sensor technology with medical models and using big data to simulate the real surgical environment, it is possible to achieve the quantitative evaluation of skill levels, such as by incorporating pressure sensors for quantitatively

evaluating operating pressure. This can create an objective evaluation method system for surgical procedures and achieve a quantitative score for surgical skills.

- (5) Three-dimensional bioprinting technology. Three-dimensional bioprinting technology can create disease models with highly simulated physiological structures by controlling the spatial arrangement of tissue cells. Many functions of the body's tissues are essential, such as the multilayer barrier function that controls transdermal drug delivery. Researchers can replicate this function by creating 3D-printed biological tissues to improve drug testing. Furthermore, bio-3D printing technology can achieve the reconstruction of human tissue organs for repairing or transplanting human tissue organs. Therefore, the development of 3D bioprinting technology can bring new breakthroughs to precision medicine.

In summary, this review focuses on the application of 3D printing technology in the medical field, particularly in medical models, surgical navigation templates, clear aligners, and human implants. However, due to the broad range of medical applications, it is not possible to cover all fields, such as drug delivery and prosthetics, which is a limitation of this article. It is crucial to note that compliance with relevant sterilization protocols is necessary for the application and experimental research of 3D printing technology in human implants and surgical navigation templates. Although there are many experimental cases throughout this article, the sterilization protocols are not explicitly explained. Nevertheless, all of the cited research examples comply with the relevant sterilization protocols. Overall, this review partially covers most of the research areas in the medical field, particularly in direct silicone 3D printing technology, which is relatively novel. This review provides readers with a clear understanding of the current applications of 3D printing technology in the medical field.

**Author Contributions:** The presented work was under supervision by W.W., S.W. and L.T.: conceptualization, Software, and Writing—original draft; S.W.: Validation, Writing—review and editing; W.Z. and J.Z.: investigation and editing; H.L. and C.H.: Validation. All authors have read and agreed to the published version of the manuscript.

**Funding:** The Guangdong Provincial Special Fund for Modern Agriculture Industry Technology Innovation Teams (2023KJ120).

**Institutional Review Board Statement:** Not applicable.

**Informed Consent Statement:** Not applicable.

**Data Availability Statement:** This study did not report any data.

**Acknowledgments:** The authors acknowledge the editors and reviewers for their constructive comments and all their support in this work.

**Conflicts of Interest:** The authors declare no conflict of interest.

## References

1. Collins, F.S.; Varmus, H. A New Initiative on Precision Medicine. *N. Engl. J. Med.* **2015**, *372*, 793–795. [[CrossRef](#)] [[PubMed](#)]
2. Wang, H.J.; Cui, Z.W.; Sun, F.; Liu, H.B.; Tang, Z.M. Superalloy GH4169 complicated components prepared by selective laser melting forming technique. *Powder Met. Technol.* **2016**, *34*, 368.
3. Sames, W.J.; List, F.A.; Pannala, S.; Dehoff, R.R.; Babu, S.S. The metallurgy and processing science of metal additive manufacturing. *Int. Mater. Rev.* **2016**, *61*, 315–360. [[CrossRef](#)]
4. Saggiomo, V.; Velders, A. Simple 3D Printed Scaffold-Removal Method for Fabrication of Intricate Microfluidic Devices. *Adv. Sci.* **2015**, *2*, 1500125. [[CrossRef](#)] [[PubMed](#)]
5. Lin, N.Y.; Homan, K.A.; Robinson, S.S.; Kolesky, D.B.; Duarte, N.; Moisan, A.; Lewis, J.A. Renal Reabsorption in 3D vascularized proximal tubule models. *Proc. Natl. Acad. Sci. USA* **2019**, *116*, 5399–5404. [[CrossRef](#)]
6. Davoodi, E.; Montazerian, H.; Haghniaz, R.; Rashidi, A.; Ahadian, S.; Sheikhi, A.; Chen, J.; Khademhosseini, A.; Milani, A.S.; Hoorfar, M.; et al. 3D-Printed Ultra-Robust Surface-Doped Porous Silicone Sensors for Wearable Biomonitoring. *ACS Nano* **2020**, *14*, 1520–1532. [[CrossRef](#)]
7. Morris, C.; Barber, R.; Day, R. Orofacial prosthesis design and fabrication using stereolithography. *Aust. Dent. J.* **2000**, *45*, 250–253. [[CrossRef](#)]

8. Wu, G.; Zhou, B.; Bi, Y.; Zhao, Y. Selective laser sintering technology for customized fabrication of facial prostheses. *J. Prosthet. Dent.* **2008**, *100*, 56–60. [[CrossRef](#)]
9. Yoshioka, F.; Ozawa, S.; Okazaki, S.; Tanaka, Y. Fabrication of an Orbital Prosthesis Using a Noncontact Three-Dimensional Digitizer and Rapid-Prototyping System. *J. Prosthodont.* **2010**, *19*, 598–600. [[CrossRef](#)]
10. Al Mardini, M.; Ercoli, C.; Graser, G.N. A technique to produce a mirror-image wax pattern of an ear using rapid prototyping technology. *J. Prosthet. Dent.* **2005**, *94*, 195–198. [[CrossRef](#)]
11. Chandra, A.; Watson, J.; Rowson, J.; Holland, J.; Harris, R.; Williams, D. Application of rapid manufacturing techniques in support of maxillofacial treatment: Evidence of the requirements of clinical applications. *Proc. Inst. Mech. Eng. Part B J. Eng. Manuf.* **2005**, *219*, 469–475. [[CrossRef](#)]
12. Reitelshofer, S.; Landgraf, M.; Graf, D.; Bugert, L.; Franke, J. A new production process for soft actuators and sensors based on dielectric elastomers intended for safe human robot interaction. In Proceedings of the 2015 IEEE/SICE International Symposium on System Integration (SII), Nagoya, Japan, 11–13 December 2015; pp. 51–56. [[CrossRef](#)]
13. McCoul, D.; Rosset, S.; Schlatter, S.; Shea, H. Inkjet 3D printing of UV and thermal cure silicone elastomers for dielectric elastomer actuators. *Smart Mater. Struct.* **2017**, *26*, 125022. [[CrossRef](#)]
14. Stieghorst, J.; Doll, T. Rheological behavior of PDMS silicone rubber for 3D printing of medical implants. *Addit. Manuf.* **2018**, *24*, 217–223. [[CrossRef](#)]
15. Liravi, F.; Vlasea, M. Powder bed binder jetting additive manufacturing of silicone structures. *Addit. Manuf.* **2018**, *21*, 112–124. [[CrossRef](#)]
16. Liravi, F.; Toyserkani, E. A hybrid additive manufacturing method for the fabrication of silicone bio-structures: 3D printing optimization and surface characterization. *Mater. Des.* **2017**, *138*, 46–61. [[CrossRef](#)]
17. Liravi, F.; Jacob-John, V.; Toyserkani, A.; Vlasea, M. A Hybrid Method for Additive Manufacturing of Silicone Structures. In Proceedings of the 2017 International Solid Freeform Fabrication Symposium, Austin, TX, USA, 7–9 August 2017; pp. 1897–1917.
18. In, E.; Walker, E.; Naguib, H.E. Novel development of 3D printable UV-curable silicone for multimodal imaging phantom. *Bioprinting* **2017**, *7*, 19–26. [[CrossRef](#)]
19. Kim, D.S.D.; Suriboot, J.; Grunlan, M.A.; Tai, B.L. Feasibility study of silicone stereolithography with an optically created dead zone. *Addit. Manuf.* **2019**, *29*, 100793. [[CrossRef](#)]
20. Liravi, F.; Toyserkani, E. Additive manufacturing of silicone structures: A review and prospective. *Addit. Manuf.* **2018**, *24*, 232–242. [[CrossRef](#)]
21. Kim, D.S.D.; Tai, B.L. Hydrostatic support-free fabrication of three-dimensional soft structures. *J. Manuf. Process.* **2016**, *24*, 391–396. [[CrossRef](#)]
22. Bhattacharjee, N.; Parra-Cabrera, C.; Kim, Y.T.; Kuo, A.P.; Folch, A. Desktop-Stereolithography 3D-Printing of a Poly (dimethylsiloxane)-Based Material with Sylgard-184 Properties. *Adv. Mater.* **2018**, *30*, 1800001. [[CrossRef](#)]
23. Wallin, T.J.; Simonsen, L.E.; Pan, W.; Wang, K.; Giannelis, E.; Shepherd, R.F.; Mengüç, Y. 3D printable tough silicone double networks. *Nat. Commun.* **2020**, *11*, 4000. [[CrossRef](#)] [[PubMed](#)]
24. Reitelshöfer, S.; Göttler, M.; Schmidt, P.; Treffer, P.; Landgraf, M.; Franke, J. Aerosol-Jet-Printing silicone layers and electrodes for stacked dielectric elastomer actuators in one processing device. In *Electroactive Polymer Actuators and Devices (EAPAD)*; SPIE: Bellingham, WA, USA, 2016.
25. Yang, H.; He, Y.; Tuck, C.; Wildman, R.; Ashcroft, I.; Dickens, P.; Hague, R. *High Viscosity Jetting System for 3D Reactive Inkjet Printing*; University of Texas at Austin: Austin, TX, USA, 2013.
26. Unkovskiy, A.; Spintzyk, S.; Brom, J.; Huettig, F.; Keutel, C. Direct 3D printing of silicone facial prostheses: A preliminary experience in digital workflow. *J. Prosthet. Dent.* **2018**, *120*, 303–308. [[CrossRef](#)] [[PubMed](#)]
27. Greenwood, T.E.; Hatch, S.E.; Colton, M.B.; Thomson, S.L. 3D printing low-stiffness silicone within a curable support matrix. *Addit. Manuf.* **2020**, *37*, 101681. [[CrossRef](#)] [[PubMed](#)]
28. Haghashtiani, G.; Qiu, K.; Sanchez, J.D.Z.; Fuenning, Z.J.; Nair, P.; Ahlberg, S.E.; Iaizzo, P.A.; McAlpine, M.C. 3D printed patient-specific aortic root models with internal sensors for minimally invasive applications. *Sci. Adv.* **2020**, *6*, eabb4641. [[CrossRef](#)]
29. Zhou, L.Y.; Gao, Q.; Fu, J.Z.; Chen, Q.Y.; Zhu, J.P.; Sun, Y.; He, Y. Multi-Material 3D Printing of Highly Stretchable Silicone Elastomer. *ACS Appl. Mater. Interfaces* **2019**, *11*, 23573–23583. [[CrossRef](#)]
30. O'bryan, C.S.; Bhattacharjee, T.; Niemi, S.R.; Balachandar, S.; Baldwin, N.; Ellison, S.T.; Taylor, C.R.; Sawyer, W.G.; Angelini, T.E. Three-dimensional printing with sacrificial materials for soft matter manufacturing. *MRS Bull.* **2017**, *42*, 571–577. [[CrossRef](#)]
31. Hinton, T.J.; Jallerat, Q.; Palchesko, R.N.; Park, J.H.; Grodzicki, M.S.; Shue, H.-J.; Ramadan, M.H.; Hudson, A.R.; Feinberg, A.W. Three-dimensional printing of complex biological structures by freeform reversible embedding of suspended hydrogels. *Sci. Adv.* **2015**, *1*, e1500758. [[CrossRef](#)]
32. Duraivel, S.; Laurent, D.; Rajon, D.A.; Scheutz, G.M.; Shetty, A.M.; Sumerlin, B.S.; Banks, S.A.; Bova, F.J.; Angelini, T.E. A silicone-based support material eliminates interfacial instabilities in 3D silicone printing. *Science* **2023**, *379*, 1248–1252. [[CrossRef](#)]
33. Casas-Murillo, C.; Zuñiga-Ruiz, A.; Lopez-Barron, R.E.; Sanchez-Uresti, A.; Gogea-coechea-Hernandez, A.; Muñoz-Maldonado, G.E.; Salinas-Chapa, M.; Elizondo-Riojas, G.; Negreros-Osuna, A.A. 3D-printed anatomical models of the cystic duct and its variants, a low-cost solution for an in-house built simulator for laparoscopic surgery training. *Surg. Radiol. Anat.* **2021**, *43*, 537–544. [[CrossRef](#)]

34. Li, A.; Tang, R.; Rong, Z.; Zeng, J.; Xiang, C.; Yu, L.; Zhao, W.; Dong, J. The Use of Three-Dimensional Printing Model in the Training of Choledochoscopy Techniques. *World J. Surg.* **2018**, *42*, 4033–4038. [[CrossRef](#)]
35. Zhang, Y.; Xia, J.; Zhang, J.; Mao, J.; Chen, H.; Lin, H.; Jiang, P.; He, X.; Xu, X.; Yin, M.; et al. Validity of a soft and flexible 3D-printed Nissen fundoplication model in surgical training. *Bioprint* **2022**, *8*, 61–69. [[CrossRef](#)]
36. Wei, F.; Wang, W.; Gong, H.; Cao, J.; Chen, J.; Chen, H.; Wang, Z. Reusable modular 3D-printed dry lab training models to simulate minimally invasive choledoch jejunostomy. *J. Gastrointest. Surg.* **2021**, *25*, 1899–1901. [[CrossRef](#)]
37. Engelhardt, S.; Sauerzapf, S.; Preim, B.; Karck, M.; Wolf, I.; De Simone, R. Flexible and comprehensive patient-specific mitral valve silicone models with chordae tendineae made from 3D-printable molds. *Int. J. Comput. Assist. Radiol. Surg.* **2019**, *14*, 1177–1186. [[CrossRef](#)]
38. Imbrie-Moore, A.M.; Paullin, C.C.; Paulsen, M.J.; Grady, F.; Wang, H.; Hironaka, C.E.; Farry, J.M.; Lucian, H.J.; Woo, Y.J. A novel 3D-Printed preferential posterior mitral annular dilation device delineates regurgitation onset threshold in an ex vivo heart simulator. *Med. Eng. Phys.* **2020**, *77*, 10–18. [[CrossRef](#)]
39. Zelis, J.M.; Meiburg, R.; Roijen, J.J.; Janssens, K.L.; van't Veer, M.; Pijls, N.H.; Johnson, N.P.; van de Vosse, F.N.; Tonino, P.A.; Rutten, M.C. 3D-printed stenotic aortic valve model to simulate physiology before, during, and after transcatheter aortic valve implantation. *Int. J. Cardiol.* **2020**, *313*, 32–34. [[CrossRef](#)]
40. Michael, B. Consequences of Malalignment in Total Knee Arthroplasty: Few if Any-Opposes. *J. Arthroplast.* **2010**, *21*, 99–101.
41. Gan, Y.; Ding, J.; Xu, Y.; Hou, C. Accuracy and efficacy of osteotomy in total knee arthroplasty with patient-specific navigational template. *Int. J. Clin. Exp. Med.* **2015**, *8*, 12192–12201.
42. Kwon, O.R.; Kang, K.T.; Son, J.; Choi, Y.J.; Suh, D.S.; Koh, Y.G. The Effect of Femoral Cutting Guide Design Improvements for Patient-Specific Instruments. *BioMed Res. Int.* **2015**, *2015*, 978686. [[CrossRef](#)]
43. Asada, S.; Mori, S.; Matsushita, T.; Nakagawa, K.; Tsukamoto, I.; Akagi, M. Comparison of MRI-and CT-based patient-specific guides for total knee arthroplasty. *Knee* **2014**, *21*, 1238–1243. [[CrossRef](#)]
44. Hafez, M.A.; Chelule, K.L.; Seedhom, B.B.; Sherman, K.P. Computer-assisted total knee arthroplasty using patient-specific templating. *Clin. Orthop. Relat. Res.* **2006**, *444*, 184–192. [[CrossRef](#)]
45. Ikram, N.; Batra, A.V. Accuracy of bone resection in total knee arthroplasty using CT assisted-3D printed patient specific cutting guides. *SICOT J.* **2018**, *4*, 29.
46. Yu, J.; Shi, Q. Efficacy Evaluation of 3D Navigational Template for Salter Osteotomy of DDH in Children. *BioMed Res. Int.* **2021**, *2021*, 8832617. [[CrossRef](#)] [[PubMed](#)]
47. Mason, A.; Paulsen, R.; Babuska, J.M.; Rajpal, S.; Burneikiene, S.; Nelson, E.L.; Villavicencio, A.T. The accuracy of pedicle screw placement using intraoperative image guidance system. *J. Neurosurg. Spine* **2014**, *20*, 196–203. [[CrossRef](#)] [[PubMed](#)]
48. Matjaz, M.; Igor, D.; Matjaz, V.; Tomaz, B.; Tomaz, F.; Gregor, R. Error rate of multilevel rapid prototyping trajectories for pedicles screw placement in lumbar and sacral sping. *Chin. J. Traumatol.* **2014**, *17*, 261–266.
49. Gelalis, I.D.; Stafilas, K.S.; Korompilias, A.V.; Zacharis, K.C.; Beris, A.E.; Xenakis, T.A. Decompressive surgery for degenerative lumbar spinal stenosis: Long-term results. *Int. Orthop.* **2006**, *30*, 256–261. [[CrossRef](#)]
50. Hu, Y.; Yuan, Z.S.; Kepler, C.K.; Albert, T.J.; Xie, H.; Yuan, J.B.; Dong, W.X.; Wang, C.T. Deviation analysis of atlantoaxial pedicle screws assisted by a drill template. *Orthopedics* **2014**, *5*, 420–427. [[CrossRef](#)]
51. Carletti, E.; Motta, A.; Migliaresi, C. Scaffolds for tissue engineering and 3D cell inter. *Methods Mol. Biol.* **2011**, *695*, 17–39.
52. Sugawara, T.; Higashiyama, N.; Kaneyama, S.; Takabatake, M.; Watanabe, N.; Uchida, F.; Sumi, M.; Mizoi, K. Multistep pedicle screw insertion procedure with patient-specific lamina fit-and-lock templates for the thoracic spine: Clinical article. *J. Neurosurg. Spine* **2013**, *19*, 185–190. [[CrossRef](#)]
53. Liang, B.; Chen, Q.; Liu, S.; Chen, S.; Yao, Q.; Wei, B.; Xu, Y.; Tang, C.; Wang, L. A feasibility study of individual 3D-printed navigation template for the deep external fixator pin position on the iliac crest. *BMC Musculoskelet. Disord.* **2020**, *21*, 478. [[CrossRef](#)]
54. Shi, W.; Aierken, G.; Wang, S.; Abuduwali, N.; Xia, Y.; Rezhake, R.; Zhao, S.; Zhou, M.; Sheng, W.; Rexiti, P. Application study of three-dimensional printed navigation template between traditional and novel cortical bone trajectory on osteoporosis lumbar spine. *J. Clin. Neurosci. Off. J. Neurosurg. Soc. Australas.* **2021**, *85*, 41–48. [[CrossRef](#)]
55. Ryu, J.-H.; Kwon, J.-S.; Jiang, H.B.; Cha, J.-Y.; Kim, K.-M. Effects of thermoforming on the physical and mechanical properties of thermoplastic materials for transparent orthodontic aligners. *Korean J. Orthod.* **2018**, *48*, 316–325. [[CrossRef](#)]
56. Tartaglia, G.M.; Mapelli, A.; Maspero, C.; Santaniello, T.; Serafin, M.; Farronato, M.; Caprioglio, A. Direct 3D Printing of Clear Orthodontic Aligners: Current State and Future Possibilities. *Materials* **2021**, *14*, 1799. [[CrossRef](#)]
57. Edelmann, A.; English, J.D.; Chen, S.J.; Kasper, F.K. Analysis of the thickness of 3-dimensional-printed orthodontic aligners. *Am. J. Orthod. Dentofac. Orthop.* **2020**, *158*, e91–e98. [[CrossRef](#)]
58. Bartkowiak, T.; Walkowiak-Śliziuk, A. 3D printing technology in orthodontics-review of current applications. *J. Stomatol.* **2018**, *71*, 356–364. [[CrossRef](#)]
59. Bagheri, A.; Jin, J. Photopolymerization in 3D Printing. *ACS Appl. Polym. Mater.* **2019**, *1*, 593–611. [[CrossRef](#)]
60. Phillips, B.T.; Allder, J.; Bolan, G.; Nagle, R.S.; Redington, A.; Hellebrekers, T.; Borden, J.; Pawlenko, N.; Licht, S. Additive manufacturing aboard a moving vessel at sea using passively stabilized stereolithography (SLA) 3D printing. *Addit. Manuf.* **2020**, *31*, 100969. [[CrossRef](#)]

61. Lo Giudice, A.; Ronsivalle, V.; Grippaudo, C.; Lucchese, A.; Muraglie, S.; Lagravère, M.O.; Isola, G. One Step before 3D Printing-Evaluation of Imaging Software Accuracy for 3-Dimensional Analysis of the Mandible: A Comparative Study Using a Surface-to-Surface Matching Technique. *Materials* **2020**, *13*, 2798. [[CrossRef](#)] [[PubMed](#)]
62. Lo Giudice, A.; Ortensi, L.; Farronato, M.; Lucchese, A.; Lo Castro, E.; Isola, G. The step further smile virtual planning: Milled versus prototyped mock-ups for the evaluation of the designed smile characteristics. *BMC Oral Health* **2020**, *20*, 165. [[CrossRef](#)]
63. Nasef, A.A.; El-Beialy, A.R.; Mostafa, Y.A. Virtual techniques for designing and fabricating a retainer. *Am. J. Orthod. Dentofac. Orthop.* **2014**, *146*, 394–398. [[CrossRef](#)]
64. Jindal, P.; Juneja, M.; Siena, F.L.; Bajaj, D.; Breedon, P. Mechanical and geometric properties of thermoformed and 3D printed clear dental aligners. *Am. J. Orthod. Dentofac. Orthop.* **2019**, *156*, 694–701. [[CrossRef](#)]
65. Zinelis, S.; Panayi, N.; Polychronis, G.; Papageorgiou, S.N.; Eliades, T. Comparative analysis of mechanical properties of orthodontic aligners produced by different contemporary 3D printers. *Orthod. Craniofacial Res.* **2022**, *25*, 336–341. [[CrossRef](#)] [[PubMed](#)]
66. McCarty, M.C.; Chen, S.J.; English, J.D.; Kasper, F. Effect of print orientation and duration of ultraviolet curing on the dimensional accuracy of a 3-dimensionally printed orthodontic clear aligner design. *Am. J. Orthod. Dentofac. Orthop.* **2020**, *158*, 889–897. [[CrossRef](#)] [[PubMed](#)]
67. Aravind Shanmugasundaram, S.; Razmi, J.; Mian, M.J.; Ladani, L. Mechanical Anisotropy and Surface Roughness in Additively Manufactured Parts Fabricated by Stereolithography (SLA) Using Statistical Analysis. *Materials* **2020**, *13*, 2496. [[CrossRef](#)] [[PubMed](#)]
68. Oladapo, B.I.; Zahedi, S.A.; Ismail, S.O.; Omigbodun, F.T. 3D printing of PEEK and its composite to increase biointerfaces as a biomedical material—A review. *Colloids Surf. B Biointerfaces* **2021**, *203*, 111726. [[CrossRef](#)]
69. Anandhapadman, A.; Venkateswaran, A.; Jayaraman, H.; Veerabadrán Ghone, N. Advances in 3D printing of composite scaffolds for the repairment of bone tissue associated defects. *Biotechnol. Prog.* **2022**, *38*, e3234. [[CrossRef](#)]
70. Han, X.; Yang, D.; Yang, C.; Spintzyk, S.; Scheideler, L.; Li, P.; Li, D.; Geis-Gerstorf, J.; Rupp, F. Carbon Fiber Reinforced PEEK Composites Based on 3D-Printing Technology for Orthopedic and Dental Applications. *J. Clin. Med.* **2019**, *8*, 240. [[CrossRef](#)]
71. Haleem, A.; Javaid, M. Polyether ether ketone (PEEK) and its manufacturing of customised 3D printed dentistry parts using additive manufacturing. *Clin. Epidemiol. Glob. Health* **2019**, *7*, 654–660. [[CrossRef](#)]
72. Deng, X.; Zeng, Z.; Peng, B.; Yan, S.; Ke, W. Mechanical Properties Optimization of Poly-Ether-Ether-Ketone via Fused Deposition Modeling. *Materials* **2018**, *11*, 216. [[CrossRef](#)]
73. Oladapo, B.I.; Zahedi, S.A.; Ismail, S.O.; Omigbodun, F.T.; Bowoto, O.K.; Olawumi, M.A.; Muhammad, M.A. 3D printing of PEEK–cHAp scaffold for medical bone implant. *Bio-Des. Manuf.* **2021**, *4*, 44–59. [[CrossRef](#)]
74. Wang, P.; Zou, B.; Ding, S.; Li, L.; Huang, C. Effects of FDM-3D printing parameters on mechanical properties and microstructure of CF/PEEK and GF/PEEK. *Chin. J. Aeronaut.* **2020**, *34*, 236–246. [[CrossRef](#)]
75. Zheng, J.; Zhao, H.; Dong, E.; Kang, J.; Liu, C.; Sun, C.; Li, D.; Wang, L. Additively-manufactured PEEK/HA porous scaffolds with highly-controllable mechanical properties and excellent biocompatibility. *Mater. Sci. Eng. C* **2021**, *2*, 112333. [[CrossRef](#)]
76. Mounir, M.; Shalash, M.; Mounir, S.; Nassar, Y.; El Khatib, O. Assessment of three dimensional bone augmentation of severely atrophied maxillary alveolar ridges using prebent titanium mesh vs customized poly-ether-ether-ketone (PEEK) mesh: A randomized clinical trial. *Clin. Implant. Dent. Relat. Res.* **2019**, *21*, 960–967. [[CrossRef](#)]
77. Kang, J.; Zhang, J.; Zheng, J.; Wang, L.; Li, D.; Liu, S. 3D-printed PEEK implant for mandibular defects repair—A new method. *J. Mech. Behav. Biomed. Mater.* **2021**, *116*, 104335. [[CrossRef](#)]
78. Chen, S.G.; Yang, J.; Jia, Y.G.; Lu, B.; Ren, L. TiO<sub>2</sub> and PEEK reinforced 3D printing PMMA composite resin for dental denture base applications. *Nanomaterials* **2019**, *9*, 1049. [[CrossRef](#)]
79. Zhang, L.C.; Klemm, D.; Eckert, J.; Hao, Y.L.; Sercombe, T.B. Manufacture by selective laser melting and mechanical behavior of a biomedical Ti–24Nb–4Zr–8Sn alloy. *Scr. Mater.* **2011**, *65*, 21–24. [[CrossRef](#)]
80. Edwards, P.; Ramulu, M. Effect of build direction on the fracture toughness and fatigue crack growth in selective laser melted Ti–6Al–4V. *Fatigue Fract. Eng. Mater. Struct.* **2015**, *38*, 1228–1236. [[CrossRef](#)]
81. Chen, L.Y.; Huang, J.C.; Lin, C.H.; Pan, C.T.; Chen, S.Y.; Yang, T.L.; Lin, D.Y.; Lin, H.K.; Jang, J.S.C. Anisotropic response of Ti–6Al–4V alloy fabricated by 3D printing selective laser melting. *Mater. Sci. Eng. A* **2017**, *682*, 389–395. [[CrossRef](#)]
82. Dekker, T.J.; Steele, J.R.; Federer, A.E.; Hamid, K.S.; Adams, S.B., Jr. Use of patient-specific 3D-printed titanium implants for complex foot and ankle limb salvage, deformity correction and arthrodesis procedures. *Foot Ankle Int.* **2018**, *8*, 916–921. [[CrossRef](#)]
83. Mobbs, R.J.; Parr, W.C.; Choy, W.J.; McEvoy, A.; Walsh, W.R.; Phan, K. Anterior Lumbar Interbody Fusion (ALIF) using a personalised approach: Is custom the future of implants for ALIF surgery? *World Neurosurg.* **2019**, *124*, 1–23. [[CrossRef](#)]
84. Belvedere, C.; Siegler, S.; Fortunato, A.; Caravaggi, P.; Liverani, E.; Durante, S.; Ensini, A.; Konow, T.; Leardini, A. New comprehensive procedure for custom-made total ankle replacements: Medical imaging, joint modeling, prosthesis design and 3D printing. *J. Orthop. Res.* **2019**, *37*, 760–768. [[CrossRef](#)]
85. Xu, L.; Qin, H.; Tan, J.; Cheng, Z.; Luo, X.; Tan, H.; Huang, W. Clinical study of 3D printed personalized prosthesis in the treatment of bone defect after pelvic tumor resection. *J. Orthop. Translat.* **2021**, *29*, 163–169. [[CrossRef](#)] [[PubMed](#)]
86. Wang, M.; Wu, Y.; Lu, S.; Chen, T.; Zhao, Y.; Chen, H.; Tang, Z. Fabrication and characterization of selective laser melting printed Ti–6Al–4V alloys subjected to heat treatment for customized implants design. *Prog. Nat. Sci. Mater. Int.* **2016**, *26*, 671–677. [[CrossRef](#)]
87. Li, J.; Chen, D.; Zhang, Y.; Yao, Y.; Mo, Z.; Wang, L.; Fan, Y. Diagonal-symmetrical and Midline-symmetrical Unit Cells with Same Porosity for Bone Implant: Mechanical Properties Evaluation. *J. Bionic Eng.* **2019**, *16*, 468–479. [[CrossRef](#)]

88. Epasto, G.; Palomba, G.; Di Bella, S.; Mineo, R.; Guglielmino, E.; Traina, F. Experimental investigation of rhombic dodecahedron micro-lattice structures manufactured by Electron Beam Melting. *Mater. Today Proc.* **2019**, *7 Pt 1*, 578–585. [[CrossRef](#)]
89. Wang, P.; Li, X.; Luo, S.; Nai, M.L.S.; Ding, J.; Wei, J. Additively manufactured heterogeneously porous metallic bone with biostructural functions and bone-like mechanical properties. *J. Mater. Sci. Technol.* **2021**, *62*, 173–179. [[CrossRef](#)]

**Disclaimer/Publisher’s Note:** The statements, opinions and data contained in all publications are solely those of the individual author(s) and contributor(s) and not of MDPI and/or the editor(s). MDPI and/or the editor(s) disclaim responsibility for any injury to people or property resulting from any ideas, methods, instructions or products referred to in the content.